THE JOURNAL OF COMPARATIVE NEUROLOGY 464:220–237 (2003)

Overlapping Distributions of Orexin/Hypocretin- and Dopamine-β-Hydroxylase Immunoreactive Fibers in Rat Brain Regions Mediating Arousal, Motivation, and Stress

BRIAN A. BALDO,[1]* ROGER A. DANIEL,[1] CRAIG W. BERRIDGE,[1,2] AND ANN E. KELLEY[1,2]

[1]Department of Psychiatry, University of Wisconsin-Madison Medical School, Madison, Wisconsin 53719

[2]Department of Psychology, University of Wisconsin-Madison, Madison, Wisconsin 53719

ABSTRACT

A double-label immunohistochemical study was carried out to investigate overlap between dopamine-β-hydroxylase (DβH) -immunopositive projections and the projections of hypothalamic neurons containing the arousal- and feeding-related peptide, orexin/hypocretin (HCRT), in rat brain. Numerous intermingled HCRT-immunopositive and DβH-immunopositive fibers were seen in a ventrally situated corridor extending from the hypothalamus to deep layers of the infralimbic cortex. Both fiber types avoided the nucleus accumbens core, caudate putamen, and the globus pallidus. In the diencephalon, overlap was observed in several hypothalamic areas, including the perifornical, dorsomedial, and paraventricular nuclei, as well as in the paraventricular thalamic nucleus. Intermingled HCRT-containing and DβH-containing fibers extended from the hypothalamus into areas within the medial and central amygdala, terminating at the medial border of the lateral subdivision of the central nucleus of the amygdala. Dense overlap between the two fiber types was also observed in the periaqueductal gray, particularly in the vicinity of the dorsal raphe, as well as (to a lesser extent) in the ventral tegmental area, the retrorubral field, and the pedunculopontine tegmental nucleus. Hypocretin-containing cell bodies, located in the perifornical and lateral hypothalamus, were embedded within a dense plexus of DβH-immunopositive fibers and boutons, with numerous cases of apparent contacts of DβH-containing boutons onto HCRT-immunopositive soma and dendrites. HCRT-containing fibers were observed amid the noradrenergic cells of the locus coeruleus, and in the vicinity of the A1, A2, and A5 cell groups. Hence, the projections of these two arousal-related systems, originating in distinctly different parts of the brain, jointly target several forebrain regions and brainstem monoaminergic nuclei involved in regulating core motivational processes. J. Comp. Neurol. 464: 220–237, 2003.

Indexing terms: norepinephrine; hypothalamus; locus coeruleus; extended amygdala; behavioral state

It is well-established that central noradrenergic systems participate in the neural control of arousal, attention, and behavioral state (Foote et al., 1980; Foote and Morrison, 1987). For example, electrophysiological studies have demonstrated that discharge rates of locus coeruleus neurons, the principal source of norepinephrine in the forebrain, are positively related to electroencephalographic (EEG) and behavioral indices of arousal both across the sleep–wake cycle and within the waking state (Hobson et al., 1975; Foote et al., 1980; Aston-Jones and Bloom, 1981a). Moreover, pharmacologic manipulations

Grant sponsor: National Institute on Drug Abuse (A.E.K., C.W.B.); Grant number: DA-09311; Grant number: DA-04788; Grant number: DA-10681; Grant number: DA-00389; Grant sponsor: National Institute of Mental Health (B.A.B., C.W.B.); Grant number: MH-12626; Grant number: MH-62359.

*Correspondence to: Brian A. Baldo, Department of Psychiatry, University of Wisconsin-Madison Medical School, 6001 Research Park Blvd., Madison, WI 53719. E-mail: babaldo@facstaff.wisc.edu

Received 31 January 2002; Revised 13 March 2003; Accepted 9 April 2003

DOI 10.1002/cne.10783

Published online the week of July 28, 2003 in Wiley InterScience (www.interscience.wiley.com).

Abbreviations

12	hypoglossal nucleus
3V	third ventricle
7n	facial nerve
ac	anterior commissure
aca	anterior commissure, anterior part
AcbC	nucleus accumbens core
AcbSh	nucleus accumbens shell
ACo	anterior cortical amygdaloid nucleus
AH	anterior hypothalamic area
AOP	anterior olfactory nucleus, posterior part
AP	area postrema
Aq	aqueduct
Arc	arcuate nucleus
AVDM	anteroventral thalamic nucleus, dorsomedial part
BIC	nucleus of the brachium of the inferior colliculus
BLA	basolateral amygdaloid nucleus, anterior part
BLP	basolateral amygdaloid nucleus, posterior part
BLV	basolateral amygdaloid nucleus, ventral part
BMA	basomedial amygdaloid nucleus, anterior part
BMP	basomedial amygdaloid nucleus, posterior part
BSTIA	bed nucleus of the stria terminalis, intra-amygdaloid division
BSTL	bed nucleus of the stria terminalis, lateral division
BSTM	bed nucleus of the stria terminalis, medial division
BSTMA	bed nucleus of the stria terminalis, medial division, anterior part
CeC	central amygdaloid nucleus, capsular part
CeL	central amygdaloid nucleus, lateral division
CeM	central amygdaloid nucleus, medial division
Cl	claustrum
CM	central medial thalamic nucleus
cp	cerebral peduncle
CPu	caudate/putamen
D3V	dorsal third ventricle
DEn	dorsal endopiriform nucleus
DLG	dorsal lateral geniculate nucleus
DMD	dorsomedial nucleus of the hypothalamus, dorsal part
DP	dorsal peduncular cortex
DpMe	deep mesencephalic nucleus
DR	dorsal raphe
DβH	dopamine β hydroxylase
ec	external capsule
f	fornix
Gi	gigantocellular reticular nucleus
GP	globus pallidus
HCRT	orexin/hypocretin
HDB	nucleus of the horizontal limb of the diagonal band
ic	internal capsule
icp	inferior cerebellar peduncle
IL	infralimbic cortex
InfCol	inferior colliculus
IO	inferior olive
IPAC	interstitial nucleus of the posterior limb of the anterior commissure
IPACL	IPAC, lateral part
IRt	intermediate reticular nucleus
KF	Kölliker-Fuse nucleus
LaDL	lateral amygdaloid nucleus, dorsolateral part
LaVL	lateral amygdaloid nucleus, ventrolateral part
LaVM	lateral amygdaloid nucleus, ventromedial part
LC	locus coeruleus
LGP	lateral globus pallidus
LH	lateral hypothalamic area
LHb	lateral habenular nucleus
LPGi	lateral paragigantocellular nucleus
LPO	lateral preoptic area
LRt	lateral reticular nucleus
LSD	lateral septal nucleus, dorsal part
LSI	lateral septal nucleus, intermediate part
LV	lateral ventricle
mcp	middle cerebellar peduncle
MCPO	magnocellular preoptic nucleus
MD	mediodorsal thalamic nucleus
MdD	medullary reticular nucleus, dorsal part
Me5	mesencephalic trigeminal nucleus
MeAD	medial amygdaloid nucleus, anterodorsal part
MePV	medial amygdaloid nucleus, posteroventral part
MG	medial geniculate nucleus
MHb	medial habenular nucleus
ml	medial lemniscus
MM	medial mamillary nucleus
Mo5	motor trigeminal nucleus
mp	mamillary peduncle
MPA	medial preoptic area
MS	medial septum
mt	mamillothalamic tract
MTu	medial tuberal nucleus
MVePC	medial vestibular nucleus, parvicellular part
opt	optic tract
ox	optic chiasm
Pa	paraventricular nucleus of the hypothalamus
PCRt	parvicellular reticular nucleus
PF	parafascicular thalamic nucleus
PH	posterior hypothalamic area
PLd	paralambdoid septal nucleus
PMV	premamillary nucleus, ventral part
Pn	pontine reticular nucleus
PnC	pontine reticular nucleus, caudal part
PnV	pontine reticular nucleus, ventral part
PPTg	pedunculopontine tegmental nucleus
PrC	precommissural nucleus
PrL	prelimbic cortex
Pr5	principal sensory trigeminal nucleus
PSTh	parasubthalamic nucleus
PT	parataenial thalamic nucleus
PV	paraventricular thalamic nucleus
PVA	paraventricular thalamic nucleus, anterior part
PVP	paraventricular thalamic nucleus, posterior part
py	pyramidal tract
Re	reuniens thalamic nucleus
Rh	rhomboid thalamic nucleus
RRF	retrorubral field
s5	sensory root of the trigeminal nerve
SCh	suprachiasmatic nucleus
scp	superior cerebellar peduncle
SFi	septofimbrial nucleus
SHi	septohippocampal nucleus
SI	substantia innominata
SIB	substantia innominata, basal part
SID	substantia innominata, dorsal part
SIV	substantia innominata, ventral part
sm	stria medullaris of the thalamus
SNC	substantia nigra pars compacta
SNR	substantia nigra pars reticulata
SO	supraoptic nucleus
Sol	nucleus of the solitary tract
SOR	supraoptic nucleus, retrochiasmatic part
Sp5	spinal trigeminal nucleus
sp5	spinal trigeminal tract
Sp5C	spinal trigeminal nucleus, caudal part
Sp5I	spinal trigeminal nucleus, interpolar part
SpVe	spinal vestibular nucleus
SPO	superior paraolivary nucleus
st	stria terminalis
STh	subthalamic nucleus
SubB	subbrachial nucleus
SubCD	subcoeruleus nucleus, dorsal part
SubCV	subcoeruleus nucleus, ventral part
SuM	supramammillary nucleus
SupCol	superior colliculus
VLG	ventral lateral geniculate nucleus
VMH	ventromedial nucleus of the hypothalamus
VO	ventral orbital cortex
VP	ventral pallidum
VPM	ventral posteromedial thalamic nucleus
VRe	ventral reuniens thalamic nucleus
VTA	ventral tegmental area
ZI	zona incerta

that increase firing rates of locus coeruleus neurons, or that stimulate postsynaptic noradrenergic receptors, increase cortical EEG patterns and behavioral concomitants of alert waking (Berridge and Foote, 1991, 1996; Berridge and O'Neill, 2001). In addition to arousal-related changes in the tonic activity of locus coeruleus cells, there are phasic changes, observed during alert waking states, induced by the presentation of salient stimuli (Foote et al., 1980; Aston-Jones and Bloom, 1981b). Thus, the extensive noradrenergic projection originating in the locus coeruleus participates in neural events underlying both the transition between sleeping and waking and, within waking, the processing of salient sensory information.

It was recently discovered that the hypothalamic peptide orexin/hypocretin (HCRT) also plays a crucial role in the central regulation of behavioral state. Initially, HCRT was thought to be primarily a feeding-related peptide (Sakurai et al., 1998). However, there is considerable evidence supporting a prominent role of HCRT in arousal-related processes. For example, the genetic basis for canine narcolepsy is a mutation that inactivates the hypocretin-2 receptor subtype (Lin et al., 1999). Similarly, human narcoleptics have abnormally low levels of HCRT in their cerebrospinal fluid (Nishino et al., 2000) and reduced numbers of hypothalamic HCRT-containing neurons (Thannickal et al., 2000). Ex vivo studies in rats showed that the activity of HCRT-containing neurons, as indexed by expression of the immediate early gene product Fos is positively correlated with behavioral state, such that a greater number of HCRT-containing cells express Fos in association with wakefulness (Estabrooke et al., 2001). Moreover, intraventricular infusion of HCRT increases cortical EEG indices of arousal and wakefulness in rats (Piper et al., 2000; España et al., 2001).

Given the similar state-modulatory actions of the noradrenergic and hypocretin systems, it is possible that these two systems act within a common set of neural circuits to achieve these actions. In support of this hypothesis, it has been shown both norepinephrine and HCRT increase time spent awake when injected into a circumscribed region of the basal forebrain extending from the anterior portion of the medial septum and nucleus accumbens shell to the posterior aspect of the medial preoptic area (Berridge et al., 1996; Berridge and Foote, 1996, España et al., 2001). In addition, the locus coeruleus receives a dense HCRT innervation (Peyron et al., 1998; Cutler et al., 1999; Hagan et al., 1999; Horvath et al., 1999) and HCRT acts in the vicinity of this brainstem structure to increase firing rates of locus coeruleus neurons (Hagan et al., 1999; Horvath et al., 1999; Bourgin et al., 2000). Hence, there is anatomic and physiological evidence that many of the arousal-related effects of the locus coeruleus–noradrenergic and HCRT systems are, at least in part, mediated by actions within a common set of terminal fields. Moreover, these two neurotransmitter systems display some degree of reciprocal connectivity in that the HCRT system innervates the locus coeruleus and modulates locus coeruleus–noradrenergic neurotransmission. Currently, the extent to which HCRT-synthesizing neurons receive noradrenergic innervation remains unknown.

Noradrenergic and HCRT projections target a wide range of brain regions associated with state-dependent physiological, affective, motivational, and cognitive processes. For example, as determined in separate single-label studies of these two systems, structures such as the central amygdala and bed nucleus of the stria terminalis, which have extensive connections to autonomic or endocrine effector systems and are activated by stressful environmental challenges, receive considerable noradrenergic and HCRT input. Moreover, several brain regions that mediate appetitive and reward-related processes, including the lateral hypothalamus and ventral tegmental area, contain noradrenergic and HCRT fibers, and, in the case of the lateral hypothalamus, HCRT-containing cell bodies (Fuxe et al., 1968; Swanson and Hartman, 1975; Asan, 1993; Peyron et al., 1998; Cutler et al., 1999).

Despite extensive information regarding the distribution of these two modulatory neurotransmitter systems, the extent to which they interact and regulate common substrates within their terminal fields remains unknown. It is often difficult to overlay and match fiber distributions from two different single-label studies, because the anatomic sections presented in each of the studies frequently are not directly comparable. This, in turn, can limit the detailed assessment of how closely axonal projections of two different systems co-mingle and jointly respect the same boundaries within complex structures, an important consideration given the anatomic heterogeneity of the regions targeted by the norepinephrine and HCRT systems.

Thus, the present study was undertaken to provide a detailed, systematic description of overlap between the distributions of noradrenergic and HCRT-containing axons in the rat brain, using a double-labeling technique. Our emphasis was on well-established forebrain substrates of arousal and state-dependent cognitive and affective processes. Hypocretin-containing and DβH-containing fibers were immunohistochemically labeled and stained distinguishable colors with separate peroxidase reactions. In this manner, HCRT-containing and DβH-containing axons could be directly examined in the same tissue sections. Issues of particular interest were (1) whether HCRT-containing and DβH-containing fibers jointly respect the boundaries of previously identified compartments of anatomically heterogeneous structures, (2) whether DβH-containing fibers in the hypothalamus are located in the vicinity of HCRT-containing cell bodies, and (3) whether the structures innervated by both fiber types are related either anatomically or by virtue of a common set of behavioral/physiological processes that they regulate.

MATERIALS AND METHODS

Subjects

Male Sprague-Dawley rats (Harlan, Madison, WI), each weighing 280–300 g upon arrival, were used in this study. Rats were group-housed in acrylic cages with cob bedding and maintained in a temperature and light controlled environment (12 hour light/dark cycle, lights on at 7:00 AM). Standard rat chow and slightly acidified tap water was available ad libitum. All facilities and procedures were in accordance with the guidelines regarding animal use and care put forth by the National Institutes of Health of the United States, were supervised and approved by the Institutional Animal Care and Use Committee of the University of Wisconsin, and were accredited by the Association for the Assessment and Accreditation of Laboratory Animal Care.

Histology and Immunohistochemistry

Animals (n = 4) were deeply anesthetized with sodium pentobarbital (70 mg/kg, i.p.) and perfused transcardially with heparinized saline (1 unit of heparin/ml 0.9% saline; heparin was obtained from SoloPak Laboratories, Elk Grove Village, IL), followed immediately by 500 ml of 4% paraformaldehyde in 0.01 M phosphate buffer. The brains were post-fixed in the paraformaldehyde solution overnight and subsequently taken through graded sucrose solutions (10%–20%–30% sucrose in 0.01 M phosphate-buffered saline [PBS], pH 7.3) at 4°C until the brains sank in the 30% sucrose solution (96–120 hours).

The brains were then frozen and 40-μm coronal sections were taken through the brain on a cryostat microtome. Every third section was placed into an individual well containing 0.1 M PBS with 0.1% sodium azide (pH 7.3) and stored at 5°C for at least 24 hours.

For immunohistochemical processing, sections were washed four times (10 minutes each time) in 0.01 M PBS. Endogenous peroxidase activity was inhibited by incubating slides in a quenching solution containing 10% methanol and 0.75% hydrogen peroxide in 0.01 M PBS for 10 minutes at room temperature. Sections were then washed again and incubated for 48 hours at 4°C with primary rabbit anti-rat prepro-hypocretin antibody #2050 (1:2,000, a generous gift of Dr. L. de Lecea; see Peyron et al., 1998) in an antibody dilution buffer (0.1% Triton X-100, 0.1% casein, and 0.1% sodium azide in 0.1 M PBS, pH 7.2).

After incubation, tissue was rinsed with 0.01 M PBS, and then exposed to a goat anti-rabbit biotinylated secondary antibody (Vector Laboratories, Burlingame, CA) for 2 hours. Tissue was rinsed with 0.01 M PBS, exposed to an avidin-biotin-peroxidase complex (ABC complex, Vector Laboratories) for 1 hour, rinsed again with 0.01 M PBS, and stained with diaminobenzidine (DAB, Vector Laboratories) to yield a brown precipitate.

Sections were then washed in 0.01 M PBS and exposed to a monoclonal mouse anti-rat DβH primary antibody (1:1,500, Chemicon International, Inc., Temecula, CA) diluted in the aforementioned antibody dilution buffer. Sections were exposed to the anti-DβH antibody for 48 hours at 5°C. After incubation in the anti-DβH primary antibody, sections were rinsed with 0.01 M PBS, and taken through all steps described above (except that a horse anti-mouse secondary antibody was used), omitting the quench step. Tissue was exposed to the Vector SG chromagen (Vector Laboratories), which stained DβH-containing neurons and processes a blue–gray color. Sections were mounted on Fisher Superfrost Plus slides (Fisher Scientific, Pittsburgh, PA), air-dried for 24 hours, taken through graded alcohols (95–100%), cleared in xylene for 5 days, and cover-slipped with Permount (Fisher Scientific) mounting medium.

Light microscopy and image analysis

Brightfield images in Figures 2, 3, and 5 were captured with a SPOT Diagnostics Inc. CCD camera coupled to a Leica DMR light microscope, using SPOT software version 2.2 on a PC-based microcomputer. Images in Figure 4 were captured with a Zeiss AxioCam HRC CCD camera mounted on a Zeiss AxioScope 2 light microscope, interfaced with a PC-based microcomputer. Images were imported into Adobe Photoshop, where contrast, sharpness, and color balance were modified slightly to match the actual stained tissue. Under brightfield microscopy, hypocretin-containing cell bodies and processes, which were stained with DAB, appeared brown, whereas DβH-containing processes (stained with the Vector SG chromagen) appeared blue–gray.

RESULTS

Cortex

The majority of the neocortex contained very light overlap between HCRT-containing and DβH-containing axons. A moderate-to-dense network of DβH-containing fibers was observed throughout the majority of the cortex, similar to that previously described (for review, see Foote et al., 1983). These fibers were thin and branching, and contained small, evenly spaced boutons. Scattered randomly throughout these DβH-containing fibers were a few thick, varicose HCRT-containing axons.

One notable exception to this pattern was a region extending from the ventral border of anterior infralimbic cortex, through the dorsal peduncular cortex, and into the tenia tecta (Fig. 1A). This area contained a dense collection of thick, varicose HCRT-immunopositive fibers intermingled with numerous DβH-containing axons. This dual innervation was located in the deep layers of cortex adjacent to the ventral portion of the corpus callosum and spread ventrolaterally beneath the tip of the corpus callosum to fill an area between the corpus callosum and the medial border of the anterior commissure.

Septal regions

Lateral septum. The lateral septum contained considerable overlap between HCRT- and DβH-immunopositive fibers. There was a collection of long, thin DβH-containing fibers with a few small varicosities coursing dorsally from the region of the olfactory tubercle though the lateral septum. These were likely fibers of passage ascending toward targets in the cortex or hippocampus, as described previously (see Swanson and Hartman, 1975). Dispersed among these axons were thin, branching DβH-containing fibers with numerous large boutons (Fig. 1C–E). Of interest, there was a very dense, discrete patch of these thin, varicose processes located in the central part of the lateral septum, approximately midway between midline and the lateral ventricle (Fig. 1E). Intermingled with the DβH-immunopositive elements throughout the lateral septum were numerous short, thick, HCRT-containing fibers with many large boutons. There was a patch of particularly dense HCRT innervation abutting the corpus callosum and the dorsal portion of the lateral ventricle (Fig. 1D,E).

At more posterior levels in which the fornix and the decussation of the anterior commissure were visible, the HCRT and DβH innervation of dorsal portions of the lateral septum was considerably less dense. Nevertheless, there were numerous thick, varicose HCRT-immunopositive fibers observed in the dorsolateral sectors of the septum, particularly in the zone directly adjacent to the lateral ventricle (Fig. 1F). In addition, the ventral sector of the lateral septum contained a moderately dense overlap of thin DβH-containing processes and thick, HCRT-immunopositive axons (Fig. 1F).

Medial septum/diagonal band. The entire anteroposterior extent of the diagonal band and the medial septum contained moderate to high densities of overlapping

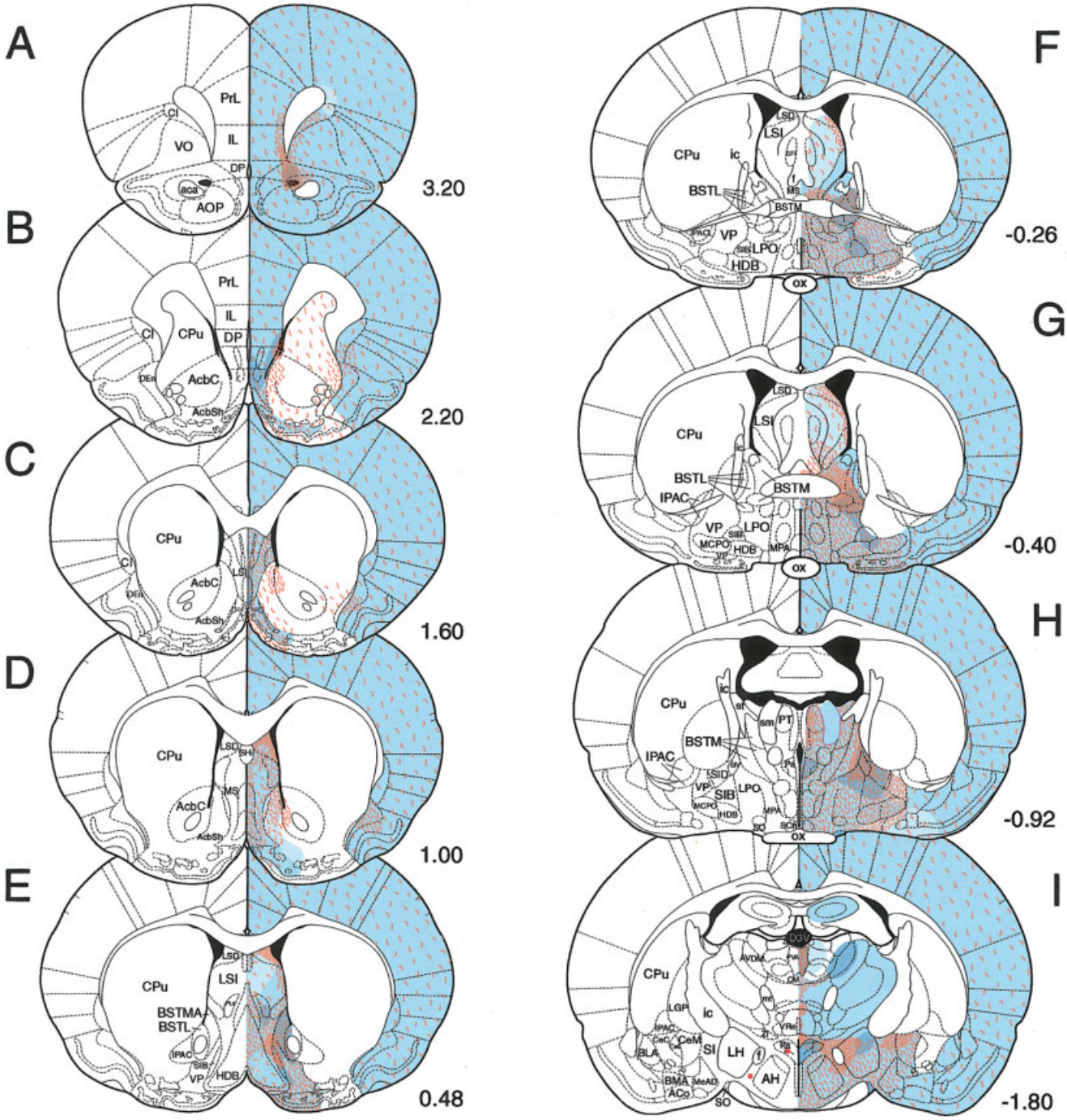

Fig. 1. **A–U:** Chartings representing anatomic distributions and relative densities of orexin/hypocretin (HCRT) -immunopositive and dopamine-β-hydroxylase (DβH) -immunopositive fibers in the rat brain. HCRT-containing axonal processes are shown as orange-colored representations of axonal fibers, and areas containing DβH-containing processes are mapped out with a solid blue color. For both neuromodulator systems, regional fiber densities are depicted as largely absent, light, moderate, or heavy, as indicated in the key. HCRT-containing cell bodies are indicated by small red circles and DβH-containing cell bodies by small blue squares; each circle or square represents approximately four cells. Coronal brain sections and labels were adapted from the atlas of Paxinos and Watson (1998). Numbers indicate distance in millimeters from bregma. For abbreviations, see list.

HCRT-containing and DβH-containing fibers. This dual HCRT/ DβH innervation mainly skirted the nucleus accumbens shell, thereby delineating the medial border of this structure, although a few fibers crossed into the nucleus accumbens shell (Fig. 1B,C). The density of HCRT-containing fibers was particularly heavy in the dorsome-

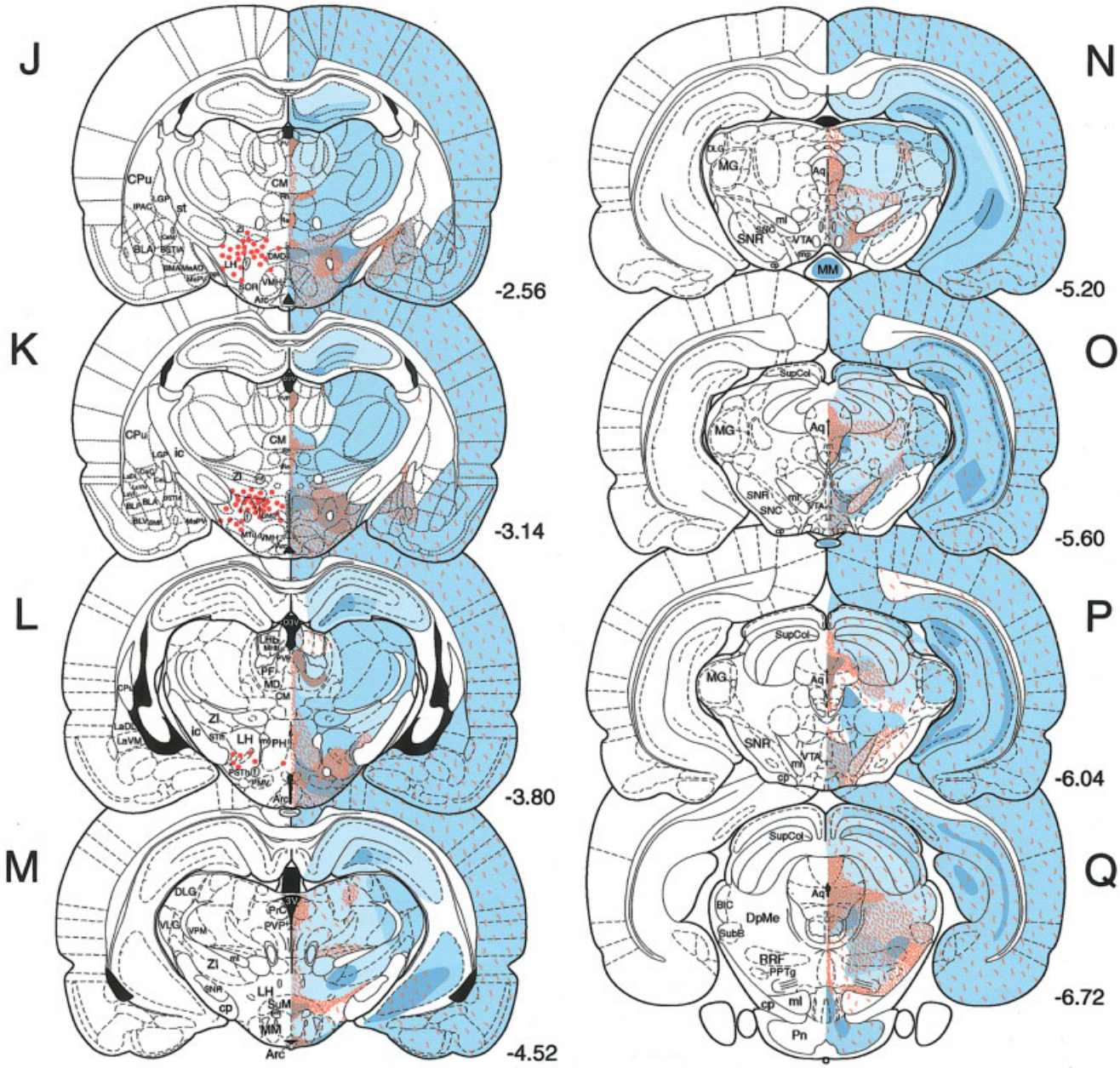

Figure 1 (Continued)

dial portions of the diagonal band and medial septum and somewhat lighter in the ventrolateral sector of the diagonal band. At the level of the decussation of the anterior commissure, moderate to heavy distributions of thin DβH-containing fibers with large boutons intermingled with thick, varicose HCRT-containing fibers were observed in the most ventromedial portion of the medial septum, immediately ventral to the fornix (Fig. 1F).

Basal ganglia

Caudate putamen and globus pallidus. The caudate putamen was mostly devoid of HCRT- or DβH-containing fibers. Two exceptions were the anterior caudate putamen and the ventrolateral striatum. The anterior caudate putamen contained a low density of long, varicose HCRT-containing fibers (Fig. 1B). The ventrolateral sector of the striatum contained a moderately dense patch of HCRT-containing fibers. This innervation, consisting of thick, branching axons with numerous large boutons, appeared to be associated with a collection of HCRT-immunopositive fibers located immediately lateral to the striatum within the claustrum and deep layers of surrounding cortex (Fig. 1C). These fibers spread medially across and underneath the ventral tip of the corpus callo-

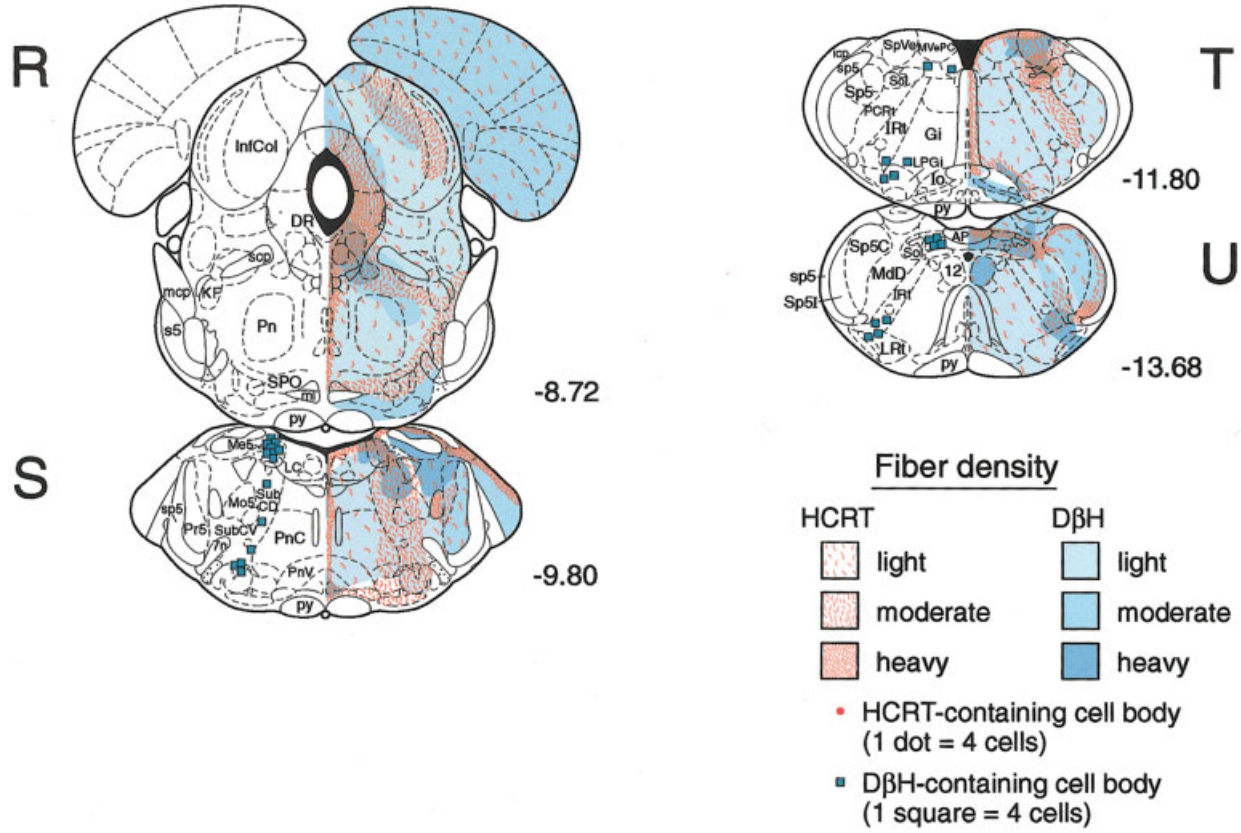

Figure 1 (Continued)

sum to innervate the striatum. Apart from these two areas, only a very few randomly scattered HCRT- or DβH-containing fibers were noted in the caudate putamen. Similarly to the caudate putamen, the globus pallidus contained few, sparsely distributed HCRT- or DβH-containing fibers (Fig. 1G,H).

Nucleus accumbens and ventral pallidum. The most anterior sectors of the nucleus accumbens contained very few HCRT- or DβH-immunopositive fibers. Proceeding caudally, the HCRT innervation grew progressively denser in two areas: the most medial aspects of the shell, and the region of the nucleus accumbens directly ventral to the lateral ventricle (Fig. 1B,C). In the medial shell, HCRT-containing fibers were interspersed with DβH-immunopositive axons; the density of both fiber types was light in the middle of the anteroposterior extent of the accumbens and became progressively heavier as one proceeded caudally. The intermingled HCRT and DβH innervation of the medial shell appeared to represent a continuation of the dense innervation of the medial septum/diagonal band area by these two fiber types (Figs. 1B,C, 2B).

The density of both HCRT-immunopositive and DβH-immunopositive fibers increased dramatically in the caudal nucleus accumbens, and particularly in the transition zone between the nucleus accumbens and the bed nucleus of the stria terminalis. Within the caudal shell, there were many thin, branching DβH-containing fibers with large boutons; these fibers were especially dense in two bands following the medial boundaries of the accumbens shell and ventral pallidum (Fig. 2E; see also Zaborszky and Cullinan, 1996; Berridge et al., 1997; Delfs et al., 1998). In the transition zone between the nucleus accumbens and the bed nucleus of the stria terminalis, the DβH-immunopositive fibers were most dense in a crescent-shaped zone outlining the medial edge of the anterior commissure and thinned somewhat, although still remaining quite dense, medially toward and within the ventral pallidum (Fig. 1E). The DβH immunoreactivity was intermingled with thick- and thin-gauge HCRT-containing fibers with many large boutons. This dual innervation was largely absent from the nucleus accumbens core, caudate putamen, and interstitial nucleus of the posterior limb of the anterior commissure; these regions presented as a homogeneous area containing a few, randomly dispersed fibers (Figs. 1C–E, 2A).

Bed nucleus of the stria terminalis and substantia innominata

The bed nucleus of the stria terminalis contained among the highest levels of HCRT/DβH overlap of any structure in the brain. A dense network of highly arborized DβH-immunoreactive fibers with many large boutons was observed in the bed nucleus of the stria terminalis, with the highest concentrations of fibers located in the ventral portion of this nucleus (Figs. 1F,G, 2C). Indeed, the DβH

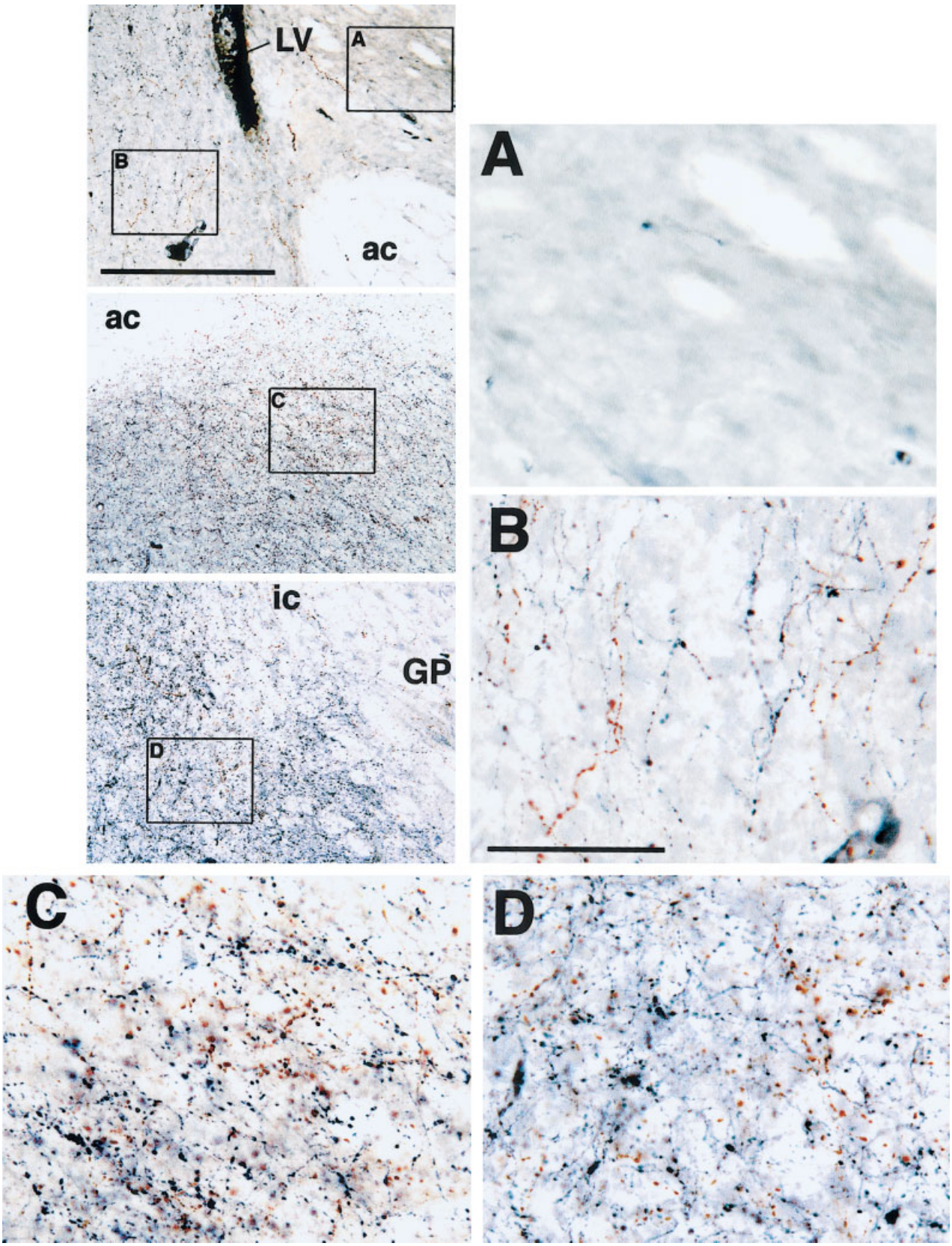

Fig. 2. Brightfield images depicting lack of HCRT- and DβH-containing fibers in the nucleus accumbens core (**A**), and intermingled HCRT- and DβH-containing fibers in the nucleus accumbens shell (**B**), bed nucleus of the stria terminalis (**C**), and dorsal substantia innominata (**D**). A–D are higher-magnification images of the boxed areas depicted in the three photomicrographs in the left column. A,B: Areas found on the section on Figure 1D. C,D: Areas seen on sections 1G and 1H, respectively. HCRT-immunopositive axons, stained with diaminobenzidine, appear reddish–brown, whereas DβH-immunoreactive elements, stained with the Vector SG chromagen, appear bluish–gray. For abbreviations, see list. Scale bars = 600 μm in the top photomicrograph in the left column (applies to all three photomicrographs in the left column), 125 μm in B (applies to A–D).

staining in this region was sufficiently intense as to be plainly apparent to the naked eye, and appeared in the microscope as a dense plexus of immunoreactive boutons. Dorsal to the anterior commissure, the DβH innervation thinned somewhat, although still remaining quite dense. Distributed throughout the bed nucleus of the stria terminalis, and intermingled with DβH-containing elements both dorsal and ventral to the anterior commissure, were numerous varicose, branching HCRT-immunoreactive processes. At more anterior levels, these fibers were particularly heavily concentrated in the dorsal regions of the bed nucleus of the stria terminalis, in a triangle-shaped territory bounded by the anterior commissure and the internal capsule (Fig. 1F); the axons in this subregion appeared to be contiguous with the HCRT innervation of the most caudal aspect of the nucleus accumbens. There were also considerable numbers of HCRT-containing fibers distributed throughout the dense patch of DβH immunoreactivity in the ventral bed nucleus of the stria terminalis (Figs. 1F,G, 2C); these axons were typically thick with many large boutons.

The dense DβH innervation of the ventral bed nucleus of the stria terminalis appeared to be contiguous with a heavy patch of immunopositive fibers and boutons visible at more posterior levels in the ventral part and sections of the basal part of the substantia innominata (Fig. 1F,G; see also Chang, 1989). Within the substantia innominata, there was considerable overlap of these DβH fibers with thick, varicose HCRT-containing axons, particularly in the zone abutting the medial border of the globus pallidus, where the anterior portion of the internal capsule was visible (Figs. 1G,H, 2D). This dual innervation dropped off sharply within the globus pallidus, thereby distinctly defining the globus pallidus/substantia innominata boundary.

Starting in the dense patch of DβH-immunoreactive boutons in the substantia innominata and continuing dorsally along the medial perimeter of the globus pallidus and anterior portion of the internal capsule, many long, thin DβH-containing fibers, likely fibers of passage, were observed. Intermingled with these axons were long, thin, varicose HCRT-containing fibers oriented in parallel to the DβH-containing axons.

In the basal substantia innominata, the dual HCRT/DβH innervation was less dense. A light distribution of HCRT-containing fibers was noted in this region, intermixed with a moderate density of DβH-immunopositive elements.

Hypothalamus

Both HCRT-immunoreactive and DβH-innunoreactive axons were present in abundance in the medial and lateral preoptic areas (Fig. 1F–H). The HCRT and DβH innervation of these regions appeared to be contiguous with, albeit somewhat less dense than, the innervation of the bed nucleus of the stria terminalis. This dual innervation extended ventrally to the base of the brain, although the density of HCRT-containing fibers was somewhat lighter in the suprachiasmatic nucleus relative to adjacent regions of the medial preoptic area. The supraoptic nucleus was heavily innervated by DβH-immunopositive fibers but contained only a few scattered HCRT-containing axons (Fig. 1H).

Hypocretin-containing cell bodies were observed in the hypothalamus, concentrated mainly in the perifornical and lateral hypothalamus, with a few cells scattered anteromedially in the paraventricular nucleus, and ventrolaterally in the medial tuberal area (Fig. 1I–L; see also Peyron et al., 1998; Sakurai et al., 1998). The hypocretin-containing cell bodies in the perifornical area were embedded within a dense collection of DβH-containing fibers likely originating in the segment of the principal adrenergic bundle that passes through the zona incerta, from where it sends a branch laterally to innervate the paraventricular nucleus and ventral aspect of the dorsomedial nucleus (Swanson and Hartman, 1975). Accordingly, we noted smooth, thin DβH-containing fibers, collected into discrete fascicular bundles (consistent with fibers of passage), in the vicinity of the zona incerta and internal capsule. Emanating from these bundles was a dense swath of DβH-immunopositive fibers and boutons spanning the hypothalamus from the zona incerta, through the hypocretin cell body-rich perifornical area and medial aspect of the lateral hypothalamus, to the paraventricular nucleus (and at more posterior levels, the dorsal portion of the dorsomedial nucleus; Fig. 1J,K). At more caudal levels, this network of DβH immunoreactivity extended ventrally into the ventromedial hypothalamic area and the medial tuberal nucleus. Within these regions, the DβH-containing fibers were thin, highly arborized, and contained many large boutons, features indicative of terminal fields. In many cases, there was the impression of synaptic contacts between hypocretin cell bodies and DβH-containing fibers and boutons (Fig. 4A–D).

There was considerable overlap between hypocretin-containing and DβH-containing fibers in a hypothalamic zone located between the paraventricular nucleus and the perifornical area. The paraventricular nucleus itself (as mentioned above) contained a very dense plexus of DβH-immunoreactive boutons; the staining in this region was so intense that it could be seen with the naked eye (Figs. 1H,I, 5A). Thick, varicose hypocretin-containing axons originating in the perifornical area were also seen in the paraventricular nucleus intermingled with the DβH-containing boutons; these hypocretin fibers were most heavily concentrated in the dorsomedial portion of this structure, in a region directly above the third ventricle, although there were also considerable numbers of fibers distributed throughout the rest of the nucleus (Figs. 1H,I, 5A). At more posterior levels, considerable overlap of hypocretin-containing and DβH-containing fibers was noted in the dorsomedial hypothalamic nucleus, especially in the lateral portion of this nucleus (Fig. 1J,K); this dual innervation appeared to be contiguous with the dense concentration of hypocretin- and DβH-immunopositive fibers in the perifornical area.

Extending laterally from the fornix, moderate to heavy concentrations of intermingled hypocretin-containing and DβH-containing fibers were observed in an area extending through the lateral hypothalamus and traversing the zone between the internal capsule and optic tract toward targets in the amygdala (Fig. 1I,J). Many of the hypocretin-containing fibers in this region, particularly those directly adjacent to the optic tract, were smooth, thin, and oriented in a parallel manner, suggestive of fibers of passage. The DβH-immunoreactive fibers in this hypothalamus/amygdala transition zone were varicose and arborized, compatible with terminal field morphology. Ventral hypothalamic structures, such as the ventromedial nucleus and the arcuate nucleus, contained moderate densities of

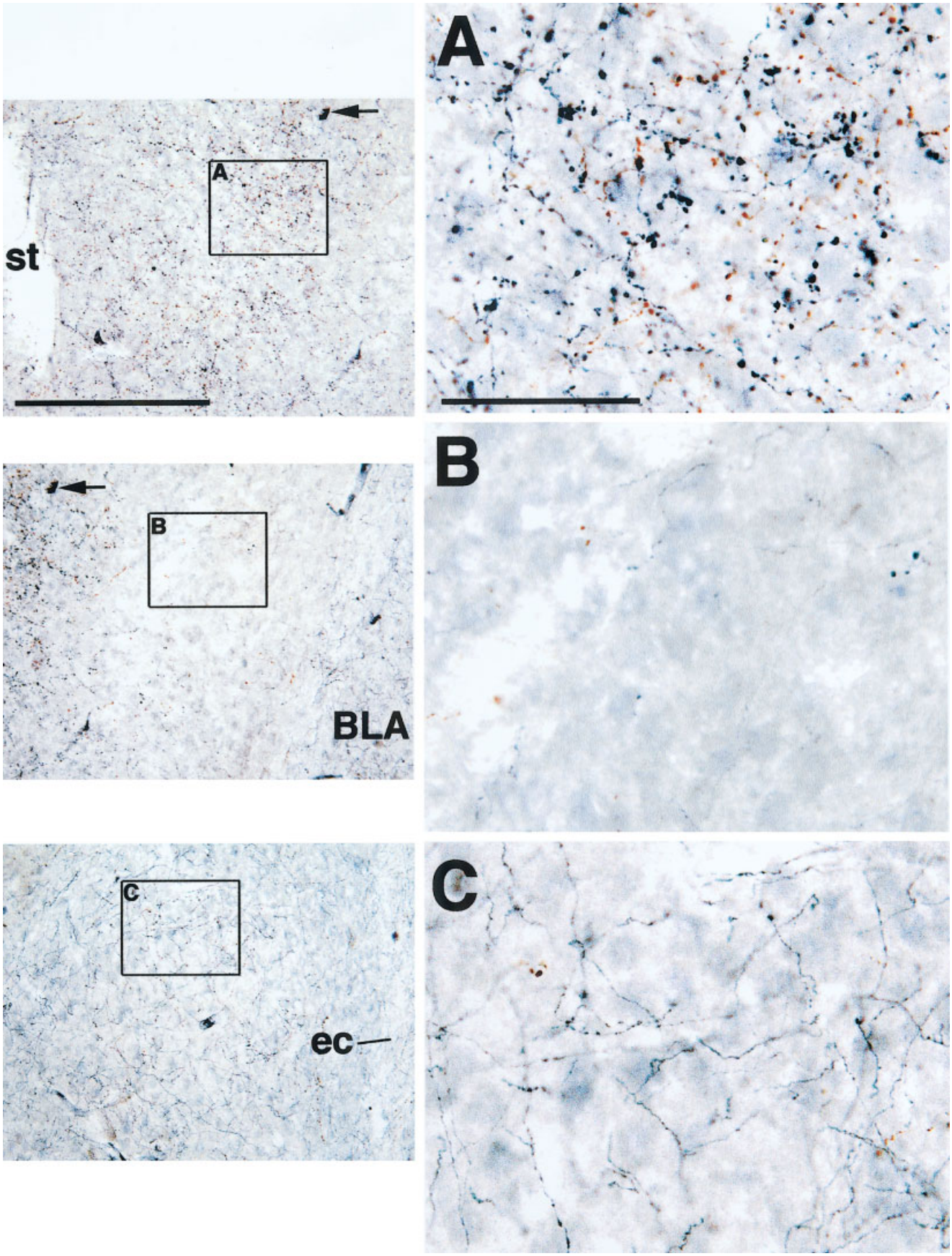

Fig. 3. Brightfield images depicting diverse HCRT- and DβH-containing fiber distributions and morphologies in the medial (top left, A) and lateral (middle left, B) subdivisions of the central amygdaloid nucleus and in the basolateral complex (bottom left, C). **A–C:** Higher-magnification images of the boxed areas in the three photomicrographs in the left column represent areas found within the amygdala on the section shown in Figure 1J. HCRT-immunopositive axons, stained with diaminobenzidine, appear reddish–brown, whereas DβH-immunoreactive elements, stained with the Vector SG chromagen, appear bluish–gray. Arrows in the top and middle photomicrographs of the left column point to the same histologic feature. For abbreviations, see list. Scale bars = 600 μm in the top photomicrograph in the left column (applies to all three photomicrographs in that column), 125 μm in A (applies to A–C).

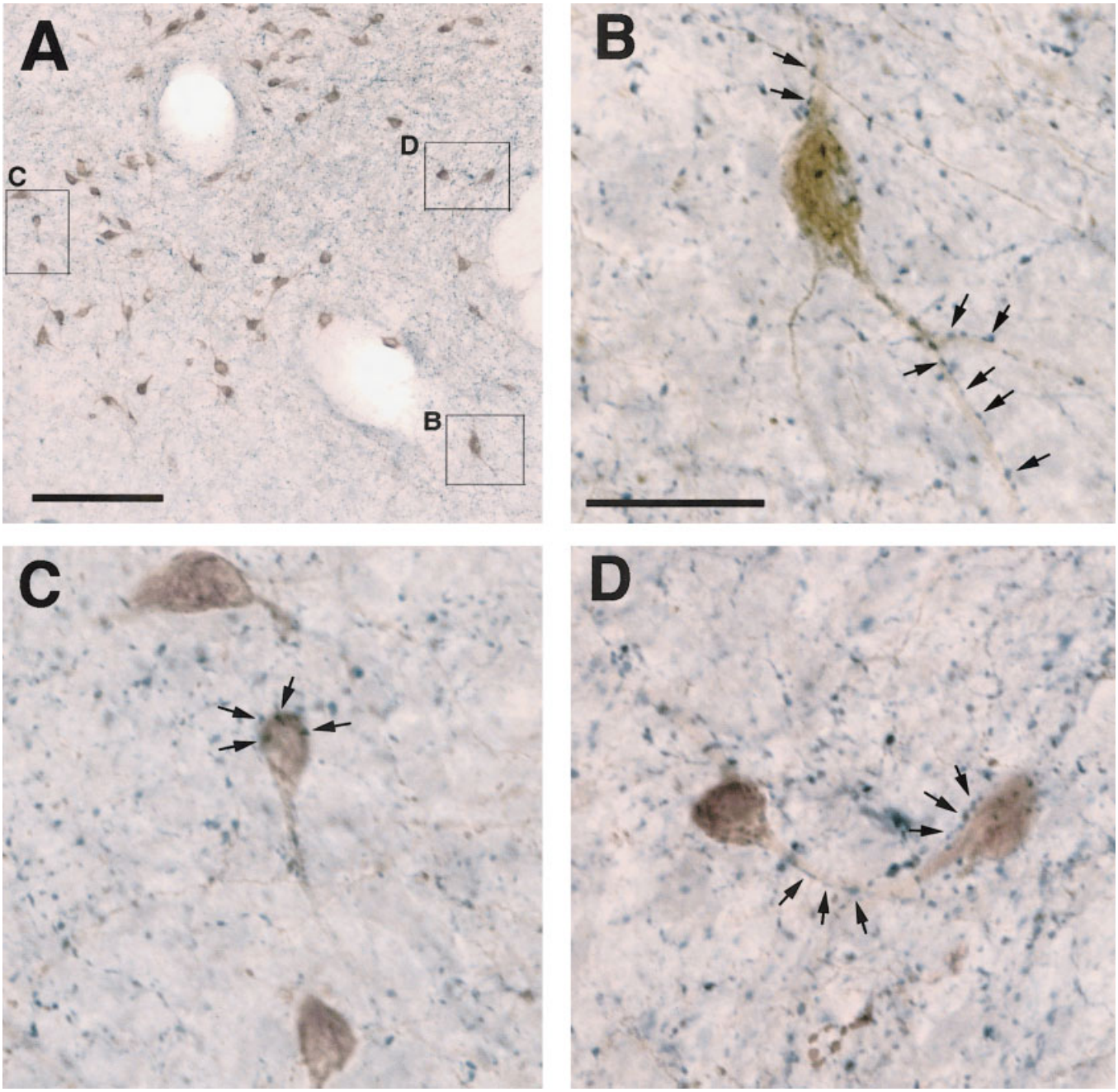

Fig. 4. **A–D:** Brightfield images showing apparent contacts (indicated by arrows) of DβH-immunoreactive boutons onto HCRT-containing soma and dendrites. HCRT-containing neurons appear brown, and DβH-containing fibers and boutons appear blue–gray. The boxed areas in A are shown at higher magnification in B, C, and D. Scale bars = 150 μm in A, 37.5 μm in B (applies to B–D).

hypocretin-containing axons, but moderate-to-light densities of DβH-immunoreactive fibers (Fig. 1K,L).

Thalamus

There was little overlap between HCRT-containing and DβH-containing fibers within the thalamus. The notable exception to this pattern was the paraventricular thalamic nucleus, which contained among the highest levels of HCRT/DβH overlap in the entire brain. Both fiber systems respected the lateral borders of the paraventricular thalamic nucleus to a striking degree; the neighboring habenular structures contained only scattered HCRT- or DβH-immunoreactive axons (Figs. 1I–K, 5).

The source of HCRT-immunopositive axons in the paraventricular nucleus of the thalamus was a collection of thick, varicose HCRT-containing axons coursing dorsally

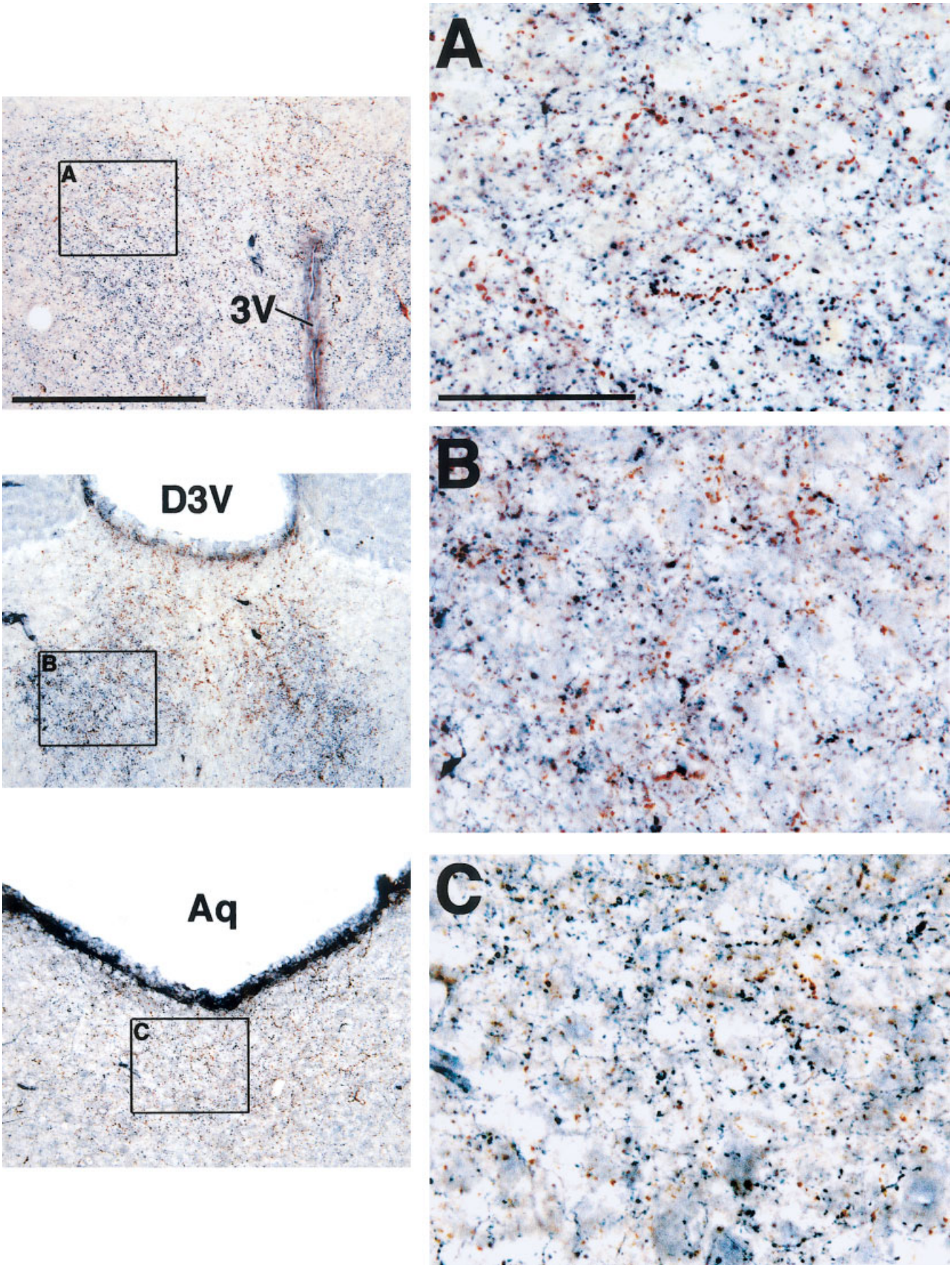

Fig. 5. Brightfield images depicting HCRT- and DβH-containing fibers in the paraventricular nucleus of the hypothalamus (top left, A), the paraventricular thalamic nucleus (middle left, B), and the posterior ventral periaqueductal gray, in the vicinity of the dorsal raphe (bottom left, C). **A–C:** Higher-magnification images of the boxed areas indicated in the three photomicrographs in the left column depict areas found on the sections shown in Figure 1I, 1K, and 1R, respectively. HCRT-immunopositive axons, stained with diaminobenzidine, appear reddish–brown, whereas DβH-immunoreactive elements, stained with the Vector SG chromagen, appear bluish–gray. For abbreviations, see list. Scale bars = 600 μm in the top photomicrograph in the left column (applies to all the photomicrographs in that column), 125 μm in A (applies to A–C).

along the midline, spanning the diencephalon from the dorsal portion of the paraventricular nucleus of the hypothalamus up to the base of the dorsal third ventricle (Fig. 1J,K). A segment of this projection branched off to follow the ventral contour of the centromedial thalamic nucleus, whereas the remainder of the fibers continued dorsally to fill, at more anterior levels, the parataenial nucleus (Fig. 1H), and further caudally, the paraventricular thalamic nucleus (Figs. 1I–K, 5B). The HCRT-containing fibers were interdigitated with the two heavy patches of DβH immunoreactivity within the paraventricular thalamic nucleus. These DβH-containing fibers were highly arborized and varicose, giving the impression at lower magnifications of homogeneous, densely packed immunoreactive boutons concentrated in bilateral oval-shaped patches within the paraventricular thalamic nucleus (Fig. 5B). At more posterior levels, the dual HCRT/DβH innervation of the paraventricular nucleus extended ventrolaterally into the region of the mediodorsal nucleus (Fig. 1L).

The remainder of the thalamus contained very few hypocretin-containing fibers, and a thin distribution of very fine DβH-containing fibers. The dorsomedial part of the anteroventral thalamic nucleus contained a dense plexus of DβH-immunopositive axons (Fig. 1I); however, HCRT-containing fibers were largely absent from this region.

Amygdala

The distributions and morphologies of DβH- and HCRT-containing fibers varied considerably among the subregions of the amygdala. A moderately dense network of intermingled HCRT- and DβH-immunoreactive fibers was observed extending laterally from the hypothalamus, traversing the hypothalamus/amygdala transition zone, and arching over the optic tract to innervate the amygdaloid division of the bed nucleus of the stria terminalis, the medial subdivision of the central nucleus (Fig. 1I,J), and, to a lesser extent, the medial amygdaloid nucleus. Both the HCRT-containing and the DβH-containing fibers in these regions were arborized and contained numerous boutons, resembling fibers seen, for example, in the bed nucleus of the stria terminalis and the dorsal substantia innominata. This heavy dual innervation ended at the medial border of the lateral subdivision of the central nucleus, which contained only a few, scattered DβH- or HCRT-containing fibers, and was thereby similar in appearance to the overlying amygdalostriatal transition zone and the caudate putamen (Figs. 1I–K, 3A,B).

The basolateral amygdaloid complex contained a moderate density of DβH-immunopositive fibers; however, there were few HCRT-containing fibers within this structure (Figs. 1J,K, 3C). Unlike the fibers in the central and medial amygdaloid nuclei, the DβH-immunopositive axons in the basolateral complex were long, thin, and contained very small boutons. These fibers resembled those seen throughout the cortex. Scattered amid the DβH-containing fibers in the basolateral complex were a few thick, varicose HCRT-immunopositive axons.

Hippocampus

The hippocampus contained almost no overlap between hypocretin-containing and DβH-containing fibers (Fig. 1I–P). Only a very few, randomly scattered hypocretin-containing axons were observed in the hippocampus. In contrast, DβH-containing fibers were present throughout the entire hippocampus; these axons were observed to be most heavily concentrated in the dentate gyrus and, more posteriorly, adjacent to fields CA1–CA3 (see also Swanson and Hartman, 1975).

Midbrain, pons, and medulla

The periaqueductal gray contained substantial overlap between HCRT-containing and DβH-containing fibers (Fig. 1N–P). Thick, varicose HCRT-immunopositive axons were observed surrounding the cerebral aqueduct and filling the medial aspects of the ventral and lateral quadrants of the gray matter. These HCRT-containing fibers were intermingled with thin, varicose DβH-immunoreactive axons. The dorsal regions of the periaqueductal gray contained fewer HCRT-containing and DβH -containing fibers. Extending laterally from the periaqueductal gray was a strip of HCRT-immunopositive axons, which traversed the midbrain and extended into the medial aspect of the medial geniculate complex (Fig. 1O). Within this region, the HCRT-containing axons were intermingled with thin, varicose, highly arborized DβH-immunopositive fibers.

At more caudal levels, the intense HCRT innervation of the midline and ventrolateral portions of the periaqueductal gray spread more laterally. Within these sectors, particularly at more caudal levels, the thick, varicose HCRT-immunoreactive axons were intermingled with a moderate-to-heavy density of branching DβH-containing fibers with numerous prominent boutons. This overlap was particularly apparent in the vicinity of the dorsal raphe (Figs. 1Q,R, 5C). The DβH axons and terminals in these areas were associated with bilateral DβH-containing fiber bundles localized just outside the ventrolateral border of the periaqueductal gray. Interspersed through these bundles was a moderate density of HCRT innervation, part of a strip of HCRT-containing fibers extending ventrally and laterally from the periaqueductal gray. Similar to the pattern seen at more rostral levels, the density of HCRT and DβH immunoreactivity thinned somewhat in dorsal sectors of the periaqueductal gray.

Moderate overlap between HCRT-containing and DβH-containing fibers was also observed in the ventral tegmental area (Fig. 1N–P). This region contained a moderate concentration of thick, varicose HCRT-containing fibers intermingled with highly varicose and arborized DβH-immunopositive axons. The HCRT innervation of the ventral tegmental area continued laterally along the ventral contour of the medial lemniscus, partially extending into the medial lemniscus itself, as well as the paranigral nucleus, the parabrachial pigmented nucleus, and the dorsal portion of the substantia nigra pars compacta, but avoiding the substantia nigra pars reticulata (Fig. 1O,P). Thin, varicose DβH-immunopositive axons overlapped the HCRT innervation along the ventral contour of the medial lemniscus but penetrated further ventrally into the substantia nigra pars compacta than did the HCRT-containing fibers. A dense collection of DβH-immunoreactive axons was also observed arching along the dorsal contour of the medial lemniscus; there were relatively few HCRT-containing axons within this region. Moderate overlap between the two fiber types was also seen more caudally in the vicinity of the retrorubral field and pedunculopontine tegmental nucleus (Fig. 1Q).

In accordance with previous reports (Peyron et al., 1998; Cutler et al., 1999; Hagan et al., 1999; Horvath et al.,

1999), a dense concentration of HCRT-immunopositive fibers was observed intermingled with the DβH-immunopositive noradrenergic cell bodies of the locus coeruleus. These axons were branching and varicose and were distributed throughout both the cell body-containing and dendritic regions of the locus coeruleus (Fig. 1S). Varicose HCRT-immunopositive axons were also noted in the dorsal aspect of the pontine central gray, along the boundary of the fourth ventricle. These axons were intermingled among the DβH-containing elements (both dendrites and varicose axons) extending from the locus coeruleus. Considerable overlap between the two fiber types was also noted in the parabrachial area (Fig. 1S) and in a strip extending through the subcoerulear region along the trajectory of DβH-containing cell bodies, extending between the locus coeruleus and the A5 noradrenergic group. There was a moderate-to-high density of HCRT-containing axons in this strip just lateral the DβH-containing soma, in the dendritic zones of these neurons (particularly in the vicinity of A5). Nevertheless, only a few clear instances of actual contacts onto DβH-containing dendrites or cell bodies were noted.

There was a moderate-to-dense concentration of HCRT-immunopositive fibers in the nucleus of the solitary tract, where the A2 noradrenergic neurons are found (Fig. 1T,U). The densest concentrations of these axons were located just dorsally and laterally to the A2 noradrenergic cells, with scattered fibers extending into the A2 region, and, in a few cases, making apparent contacts onto noradrenergic neurons. The A1 noradrenergic area contained only a few, randomly scattered HCRT-containing fibers (Fig. 1T,U).

DISCUSSION

Summary of results

Substantial overlap between HCRT- and DβH-containing projections was noted in the following zones: (1) a ventrally situated corridor extending rostrally from the HCRT-containing neurons in the perifornical/lateral hypothalamus through the anteroposterior extent of the forebrain (including medial hypothalamus, preoptic area, substantia innominata, bed nucleus of the stria terminalis, medial and lateral septal regions, and medial nucleus accumbens shell), penetrating into a circumscribed area in the deep layers of infralimbic and dorsal peduncular cortex; (2) a ventrally situated corridor extending caudally from the perifornical and lateral hypothalamus into midbrain structures such as the ventral tegmental area, retrorubral field, and pedunculopontine tegmental nucleus; (3) ventral portions of the central gray, particularly in the vicinity of the dorsal raphe, and, further caudally, in the mesencephalic gray and locus coeruleus; (4) a region extending laterally from the perifornical hypothalamus, over the optic tract, and into the intra-amygdaloid division of the bed nucleus of the stria terminalis and medial division of the central amygdaloid nucleus, ending abruptly at the medial border of the lateral division of this nucleus; (5) a very distinct area in the dorsal diencephalon including the parataenial, paraventricular, and mediodorsal thalamic nuclei. Except as noted above in (1), the majority of cortex contained a moderately dense network of long, thin, branching DβH-containing fibers, which were similar in morphology to those seen in the hippocampus and basolateral amygdala. Intermixed with these cortical fibers was a low density of randomly scattered, varicose HCRT-containing axons. Basal ganglia structures such as the caudate putamen, nucleus accumbens core, and globus pallidus were devoid of both fiber types. Within HCRT cell body-rich hypothalamic regions, a dense plexus of DβH-immunoreactive fibers and boutons was observed, with many cases of apparent contacts of DβH-containing boutons onto HCRT soma and dendrites.

Although densely intermingled HCRT- and DβH-immunoreactive fibers were observed in numerous brain structures (see above), the degree to which these processes contacted identical postsynaptic targets was not assessed; indeed, a general limitation of the light microscopy techniques used here is that they provide suggestive, rather than conclusive, evidence of synaptic contacts. Regardless, the present work was designed to provide a broad perspective and descriptive catalog of the neuroanatomic sites that might support functional interactions between HCRT- and norepinephrine-containing terminal fields. These data can serve as a framework to guide both electron microscopy studies, wherein more direct evidence of synaptic contacts can be obtained, as well as functional studies of HCRT/norepinephrine interactions.

Our general hypothesis was that DβH-immunoreactive elements represented components of the norepinephrine system. Norepinephrine, however, is also a substrate for the synthesis of epinephrine by means of the actions of phenylethanolamine-N-methyl-transferase (PNMT) in adrenergic neurons. Thus, the previously reported presence of PNMT immunoreactivity in structures like the paraventricular thalamic nucleus, perifornical hypothalamus, and medial amygdala (Hokfelt et al., 1984; Astier et al., 1987) raises the possibility that the DβH-containing processes in those structures represent adrenergic, rather than noradrenergic, fibers. Presently, the functional role of epinephrine in the central nervous system is not well-characterized, although it is likely that this amine exerts some of the same effects as norepinephrine, considering that its affinity for noradrenergic receptors is close to that of norepinephrine itself (Hoffman and Lefkowitz, 1995). Nevertheless, in general, DβH-containing projections in the brain vastly outnumber PNMT-containing projections (Swanson and Hartman, 1975; Hokfelt et al., 1984), indicating that the majority of DβH-immunoreactive fibers observed in the present study represented noradrenergic processes. More specifically, previous work examining the medial amygdala, stained separately in adjacent sections for DβH and PNMT, revealed greater numbers of DβH-containing fibers than PNMT-immunopositive processes (Fallon and Ciofi, 1992; Asan, 1993). This finding indicates that the majority of DβH-containing elements in the amygdala are noradrenergic, and supports the principle that ". . .levels of the earlier enzymes in the sequence of catecholamine synthesis are thought to be quite low in catecholaminergic fibers and terminals" (Fallon and Ciofi, 1992).

HCRT/DβH overlap and the extended amygdala

The present findings provide support for the notion of contiguity and common modulation among several basal forebrain structures comprising the extended amygdala (for an extensive review of extended amygdala anatomy, see Alheid et al., 1995). For example, intermingled DβH-

containing and HCRT-containing fibers were seen throughout the bed nucleus of the stria terminalis. The innervation of the lateral bed nucleus of the stria terminalis appeared contiguous with a dense collection of both fiber types in an area of the substantia innominata corresponding to the central and medial divisions of the sublenticular extended amygdala (Alheid et al., 1995). Proceeding caudally, moderate concentrations of both fiber types were noted in the medial subdivision of the central amygdaloid nucleus. However, this dual innervation terminated at the medial border of the lateral subdivision of the central amygdaloid nucleus.

This distinction between the medial and lateral subdivisions of the central nucleus is interesting in terms of ongoing debates regarding the classification and characterization of the various amygdaloid subregions. It has been argued that portions of the central and medial amygdaloid nuclei can be viewed as a specialized region of the striatum. For example, in situ hybridization for glutamic acid decarboxylase mRNA reveals an unbroken swath of neurons extending from the posterior caudate, through the amygdalostriatal transition zone, and into the central and medial divisions of the amygdala (Swanson and Petrovich, 1998). This observation is in general agreement with the present finding that the caudate putamen, amygdalostriatal transition zone, and the lateral subdivision of the central nucleus presented as a homogeneous region devoid of either HCRT- or DβH-containing fibers. Others have proposed that the projections, intrinsic connectivity, and histochemical features of central amygdala subdivisions recapitulate features of core-shell-ventral pallidum organization, with the lateral and medial subdivisions of the central nucleus nuclei displaying, respectively, "core-like" and "pallidum-like'" histochemical features and circuitry (Cassell et al., 1999). Again, this model is consistent, in a general sense, with the present observation that the medial subdivision of the central nucleus, like portions of the ventral pallidum, contains intermingled HCRT- and DβH-containing fibers, whereas the lateral subdivision, like the nucleus accumbens core, is devoid of either fiber type. Hence, the present data reveal further similarities between portions of the central amygdaloid nucleus and striatum, with regard to distributions of overlapping HCRT and DβH projections to these areas.

The basolateral amygdaloid complex displayed a strikingly different pattern of innervation relative to the central amygdala subregions described above. Dopamine-β-hydroxylase immunopositive axons in the basolateral nucleus resembled the long, thin, branching DβH-containing fibers in the cortex, but differed from the short, varicose fibers and terminal boutons seen in the medial portions of the amygdala (see also Fallon and Ciofi, 1992; Asan, 1993, 1997). Moreover, the relative densities of HCRT-containing vs. DβH-containing fibers in the basolateral nucleus of the amygdala (i.e., a moderate-to-heavy density of DβH-containing fibers but only a few, scattered HCRT-immunopositive axons) was very similar to the ratio of these two fiber types seen throughout the cortex but differed markedly from the ratio seen in the medial subdivision of the central amygdala, where both fiber types were present in abundance. Thus, the present results lend further support to the idea that the basolateral amygdala is structurally more similar to the cortex than it is to the central and medial divisions of the amygdala (McDonald, 1992; Alheid et al., 1995; Swanson and Petrovich, 1998).

Functional considerations

Perhaps the most straightforward implication of the present data is that hypocretin and norepinephrine may interact functionally within the brain regions containing overlapping projections from both systems. A comparison of the distributions of hypocretin-1 receptor mRNA, hypocretin-2 receptor mRNA, and mRNA for α-adrenergic and β-adrenergic receptors reveals that some combination of hypocretin and norepinephrine receptor subtypes is present in the main areas we identified as receiving overlapping HCRT and DβH input (Asanuma et al., 1991; Talley et al., 1996; Rosin et al., 1996; Trivedi et al., 1998; Marcus et al., 2001), supporting the idea of functional interactions between these two neuromodulators. The question then arises as to whether there is a unified set of physiological or behavioral processes subject to dual hypocretin/norepinephrine regulation that can be deduced on the basis of anatomic considerations. A review of the established functional roles of the areas most heavily innervated by the hypocretin and norepinephrine systems indicates that these structures are involved in the regulation of arousal or behavioral state, autonomic function and stress, and appetitively motivated behavior.

A compelling framework for hypocretin/norepinephrine interactions in the control of behavioral state comes from studies of EEG and behavioral measures of arousal after remote-controlled administration of either noradrenergic agonists or HCRT into the basal forebrain of sleeping rats. Infusions of either the β-adrenergic receptor agonist isoproterenol (Berridge et al., 1996), the monoamine-releaser amphetamine (Berridge et al., 1999), or HCRT peptides (España et al., 2001) into a region encompassing the medial septum, caudomedial nucleus accumbens shell, and the medial preoptic area elicited low-voltage cortical EEG patterns indicative of waking, along with increased motor activity. Examination of chartings from these studies reveals an excellent concordance between the sites most sensitive to the arousal-related effects of HCRT and norepinephrine, and the areas identified in the present work as containing moderate-to-dense concentrations of intermingled HCRT-containing and DβH-containing axons, especially the medial septal region and the medial preoptic area. It would be of considerable interest, therefore, to determine, in future studies, whether the combined administration of HCRT and norepinephrine into these sites interacts in an additive or superadditive manner in the control of behavioral state.

In addition to HCRT-norepinephrine interactions within arousal-related forebrain regions, overlapping projections from these two systems were noted within several monoaminergic nuclei within the midbrain and pons. For example, in agreement with prior studies, a dense concentration of HCRT-containing processes was observed within the locus coeruleus (Peyron et al., 1998; Cutler et al., 1999; Hagan et al., 1999; Horvath et al., 1999). We also noted considerable HCRT/ DβH overlap in the dorsal raphe and ventral tegmental area. Thus, HCRT and noradrenergic projections may interact to coordinate arousal-related dopaminergic, serotonergic, and noradrenergic input to the basal forebrain and cortex.

Because we observed that HCRT-containing cell bodies in the perifornical and lateral hypothalamus receive substantial DβH innervation (including many cases of apparent contacts of DβH-immunopositive boutons onto HCRT-

containing soma), the question arose as to whether these two systems interact reciprocally at the cell-body level. Thus, HCRT input to the A1 and A2 noradrenergic cell groups, major sources of perifornical/lateral hypothalamic norepinephrine (Woulfe et al., 1990; Aston-Jones et al., 1995), was examined. Although numerous HCRT-containing fibers were observed within the nucleus of the solitary tract, site of the A2 noradrenergic cell group, most of these HCRT fibers were in proximity to but not directly contacting DβH-containing dendrites or soma (although a few examples of apparent contacts were noted). Only scattered HCRT fibers were seen in the vicinity of the A1 region. These observations support the notion that HCRT may modulate neuronal activity in the A2 cell group by influencing local circuitry in the vicinity of the noradrenergic cell bodies, but do not form direct synapses onto these cells.

Currently, there is a strong emphasis on the roles of hypocretin and norepinephrine in arousal and sleep–wake regulation. However, an examination of the distribution of overlapping HCRT and DβH innervation indicates that these neuromodulators are well-situated to mediate autonomic and endocrine functions as well. For example, the bed nucleus of the stria terminalis, which contains among the densest concentrations of intermingled HCRT-containing and DβH-containing processes in the entire brain, projects to medullary centers such as the nucleus of the solitary tract and the parabrachial area to modulate autonomic processes (Schwaber et al., 1982; Sofroniew, 1983; Grove, 1988; Moga et al., 1989; Loewy, 1991). Moreover, there is substantial HCRT/DβH overlap in portions of the extended amygdala, which projects to the paraventricular nucleus of the hypothalamus, a well-established control center for hypothalamic–pituitary–adrenal axis regulation. The paraventricular nucleus itself contains numerous, intermingled HCRT-containing and DβH-containing fibers. As a group, these brain structures are involved in centrally mediated autonomic and endocrine responses associated with high arousal states, including stress (e.g., Henke, 1984; Gray, 1993; Pacak et al., 1995; Koob, 1999), raising the possibility that joint hypocretin/norepinephrine actions in the bed nucleus of the stria terminalis and related areas of the extended amygdala produce a stressful or aversive behavioral state. This hypothesis is supported by the observation that central infusions of hypocretin enhance stress-related behaviors like grooming, face-washing, and nonspecific chewing, beyond a simple proportional increase resulting from the arousal-enhancing actions of this peptide (España et al., 2002).

It is important to note that a role for norepinephrine/hypocretin interactions in the control of appetitive or reward-related processes cannot be ruled out. For example, substantial HCRT/DβH overlap was seen in brain regions involved in feeding, such as the lateral hypothalamus and caudomedial nucleus accumbens shell. We also observed overlap within the ventral tegmental area. Indeed, HCRT-containing cell bodies are confined to the lateral/perifornical hypothalamus suggesting a fundamental involvement, at least in a modulatory sense, in brain reward processes. Thus, taken together, our observations support a potential role for HCRT/adrenergic interactions in neural processes associated with both appetitive and aversive states.

One of the most circumscribed areas of HCRT/DβH overlap was found in the paraventricular thalamic nucleus. This region of the thalamus receives inputs from the suprachiasmatic nucleus (Watts et al., 1987) and projects to the infralimbic cortex, nucleus accumbens, lateral septum, bed nucleus of the stria terminalis, and amygdala (Moga et al., 1995; Bubser and Deutch, 1998), areas that themselves receive abundant overlapping HCRT-containing and DβH-containing projections. Based on its connectivity, it has been proposed that the paraventricular thalamic nucleus is well-situated to modulate stress-related dopaminergic activity in the forebrain (Bubser and Deutch, 1999). Interestingly, the paraventricular thalamic nucleus also contains among the highest levels of melatonin receptor binding in the brain (Weaver et al., 1989; Williams et al., 1991). On the basis of these anatomic findings, it could be hypothesized that this region of the thalamus represents a control site where circadian information is received and then relayed to basal forebrain regions that mediate adaptive behavioral state-related and motivational responses to environmental challenges. Inputs from the hypocretin and norepinephrine systems (and possibly the epinephrine system as well—see Hokfelt et al., 1984 and Astier et al., 1987) to the paraventricular nucleus are positioned to influence these circadian inputs, thereby potentially representing a means for these neuromodulators to override circadian control over basal forebrain sites relevant to motivation and arousal.

CONCLUSIONS

Although they originate in distinctly different parts of the brain, the hypocretin and norepinephrine systems both target structures implicated in an array of state-dependent physiological, cognitive, and affective processes, including those associated with appetitive and aversive motivational states. Within these regions, HCRT- and DβH-containing fibers are closely intermingled and, in several areas, respect precisely the same boundaries. There are also numerous DβH-containing fibers and boutons in close apposition to HCRT-containing cell bodies, in a manner suggestive of synaptic contacts. Conversely, HCRT-containing axons contact the noradrenergic cells of the locus coeruleus and are positioned to influence neural circuitry in the vicinity of the A2 and A5 noradrenergic cell groups. Thus, the present results provide anatomic evidence supporting coordinated hypocretin/norepinephrine actions within the brain.

ACKNOWLEDGMENTS

The authors thank Mrs. Carol Dizack for her artistic skill and assistance with the fiber chartings. We also thank Dr. Charles F. Landry for advice on the immunohistochemical procedures and for the use of his SPOT CCD imaging system, Dr. Steve Gammie for helpful insights regarding our photographic images and for the use of his AxioCam imaging system, Mr. Ken Sadeghian for technical assistance, and Dr. Luis de Lecea for the generous gift of the anti–prepro-hypocretin antibody.

LITERATURE CITED

Alheid GF, de Olmos, JS, Beltramino CA. 1995. Amygdala and extended amygdala. In: Paxinos G, editor. The rat nervous system. San Diego: Academic Press, Inc. p 495–578.

Asan E. 1993. Comparative single and double immunolabeling with antisera against catecholamine biosynthetic enzymes: criteria for the identification of dopaminergic, noradrenergic and adrenergic structures in selected rat brain areas. Histochemistry 99:427–442.

Asan E. 1997. Ultrastructural features of tyrosine-hydroxylase-immunoreactive afferents and their targets in the rat amygdala. Cell Tissue Res 288:449–469.

Asanuma M, Ogawa N, Mizukawa K, Haba K, Hirata H, Mori A. 1991. Distribution of the beta-2 adrenergic receptor messenger RNA in the rat brain by in situ hybridization histochemistry: effects of chronic reserpine treatment. Neurochem Res 16:1253–1256.

Astier B, Kitahama K, Denoroy L, Jouvet M, Renaud B. 1987. Immunohistochemical evidence for the adrenergic medullary longitudinal bundle as a major ascending pathway to the hypothalamus. Neurosci Lett 78:241–246.

Aston-Jones G, Bloom FE. 1981a. Activity of norepinephrine-containing locus coeruleus neurons in behaving rats anticipates fluctuations in the sleep-waking cycle. J Neurosci 1:876–886.

Aston-Jones G, Bloom FE. 1981b. Nonrepinephrine-containing locus coeruleus neurons in behaving rats exhibit pronounced responses to non-noxious environmental stimuli. J Neurosci 1:887–900.

Aston-Jones G, Shipley MT, Grzanna R. 1995. The locus coeruleus, A5 and A7 noradrenergic cell groups. In: Paxinos G, editor. The rat nervous system. San Diego: Academic Press. p 183–205.

Berridge CW, Foote SL. 1991. Effects of locus coeruleus activation on electroencephalographic activity in neocortex and hippocampus. J Neurosci 11:3135–3145.

Berridge CW, Foote SL. 1996. Enhancement of behavioral and electroencephalographic indices of waking following stimulation of noradrenergic beta-receptors within the medial septal region of the basal forebrain. J Neurosci 16:6999–7009.

Berridge CW, O'Neill J. 2001. Differential sensitivity to the wake-promoting actions of norepinephrine within the medial preoptic area and the substantia innominata. Behav Neurosci 115:165–174.

Berridge CW, Bolen SJ, Manley MS, Foote SL. 1996. Modulation of forebrain electroencephalographic activity in halothane-anesthetized rat via actions of noradrenergic beta-receptors within the medial septal region. J Neurosci 16:7010–7020.

Berridge CW, Stratford TL, Foote SL, Kelley AE. 1997. Distribution of dopamine beta-hydroxylase-like immunoreactive fibers within the shell subregion of the nucleus accumbens. Synapse 27:230–241.

Berridge CW, O'Neil J, Wifler K. 1999. Amphetamine acts within the medial basal forebrain to initiate and maintain alert waking. Neuroscience 93:885–896.

Bourgin P, Huitron-Resendiz S, Spier AD, Fabre V, Morte B, Criado JR, Sutcliffe JG, Henriksen SJ, de Lecea L. 2000. Hypocretin-1 modulates rapid eye movement sleep through activation of locus coeruleus neurons. J Neurosci 20:7760–7765.

Bubser M, Deutch AY. 1998. Thalamic paraventricular nucleus neurons collateralize to innervate the prefrontal cortex and nucleus accumbens. Brain Res 787:304–310.

Bubser M, Deutch AY. 1999. Stress induces Fos expression in neurons of the thalamic paraventricular nucleus that innervate limbic forebrain sites. Synapse 32:13–22.

Cassell MD, Freedman LJ, Shi C. 1999. The intrinsic organization of the central extended amygdala. Ann N Y Acad Sci 877:217–241.

Chang HT. 1989. Noradrenergic innervation of the substantia innominata: a light and electron microscopic analysis of dopamine beta-hydroxylase immunoreactive elements in the rat. Exp Neurol 104:101–112.

Cutler DJ, Morris R, Sheridhar V, Wattam TA, Holmes S, Patel S, Arch JR, Wilson S, Buckingham RE, Evans ML, Leslie RA, Williams G. 1999. Differential distribution of orexin-A and orexin-B immunoreactivity in the rat brain and spinal cord. Peptides 20:1455–1470.

Delfs JM, Zhu Y, Druhan JP, Aston-Jones GS. 1998. Origin of noradrenergic afferents to the shell subregion of the nucleus accumbens: anterograde and retrograde tract-tracing studies in the rat. Brain Res 806: 127–140.

España RA, Baldo BA, Kelley AE, Berridge CW. 2001. Wake-promoting and sleep-suppressing actions of hypocretin (orexin): basal forebrain sites of action. Neuroscience 106:699–715.

España RA, Plahn S, Berridge CW. 2002. Circadian-dependent and circadian-independent behavioral actions of hypocretin/orexin. Brain Res 943:224–236.

Estabrooke IV, McCarthy MT, Ko E, Chou TC, Chemelli RM, Yanagisawa M, Saper CB, Scammell TE. 2001. Fos expression in orexin neurons varies with behavioral state. J Neurosci 21:1656–1662.

Fallon JH, Ciofi P. 1992. Distribution of monamines within the amygdala. In: Aggleton J, editor. The amygdala: neurobiological aspects of emotion, memory, and mental dysfunction. New York: Wiley-Liss Inc. p 97–114.

Foote SL, Morrison JH. 1987. Extrathalamic modulation of cortical function. Annu Rev Neurosci 10:67–95.

Foote SL, Aston-Jones G, Bloom FE. 1980. Impulse activity of locus coeruleus neurons in awake rats and monkeys is a function of sensory stimulation and arousal. Proc Natl Acad Sci U S A 77:3033–3037.

Foote SL, Bloom FE, Aston-Jones G. 1983. Nucleus locus ceruleus: new evidence of anatomical and physiological specificity. Physiol Rev 63: 844–914.

Fuxe K, Hamberger B, Hokfelt T. 1968. Distribution of noradrenaline nerve terminals in cortical areas of the rat. Brain Res 8:125–131.

Gray TS. 1993. Amygdaloid CRF pathways. Role in autonomic, neuroendocrine, and behavioral responses to stress. Ann N Y Acad Sci 697:53–60.

Grove EA. 1988. Efferent connections of the substantia innominata in the rat. J Comp Neurol 277:347–364.

Hagan JJ, Leslie RA, Patel S, Evans ML, Wattam TA, Holmes S, Benham CD, Taylor SG, Routledge C, Hemmati P, Munton RP, Ashmeade TE, Shah AS, Hatcher JP, Hatcher PD, Jones DN, Smith MI, Piper DC, Hunter AJ, Porter RA, Upton N. 1999. Orexin A activates locus coeruleus cell firing and increases arousal in the rat. Proc Natl Acad Sci U S A 96:10911–110916.

Henke PG. 1984. The bed nucleus of the stria terminalis and immobilization-stress: unit activity, escape behaviour, and gastric pathology in rats. Behav Brain Res 11:35–45.

Hobson JA, McCarley RW, Wyzinski PW. 1975. Sleep-cycle oscillation: reciprocal discharge by two brainstem neuronal groups. Science 189: 55–58.

Hoffman BB, Lefkowitz RJ. 1995. Catecholamines, sympathomimetic drugs. In: Hardman JG, Limbird LE, Molinoff PB, Ruddon RW, Gilman AG, editors. Goodman & Gilman's; the pharmacological basis of therapeutics. New York: McGraw-Hill. p 199–248.

Hokfelt T, Johansson O, Goldstein M. 1984. Central catecholamine neurons as revealed by immunohistochemistry with special reference to adrenaline neurons. In: Bjorklund A, Hokfelt T, editors. Classical transmitters in the CNS. New York: Elsevier. p 157–276.

Horvath TL, Peyron C, Diano S, Ivanov A, Aston-Jones G, Kilduff TS, van Den Pol AN. 1999. Hypocretin (orexin) activation and synaptic innervation of the locus coeruleus noradrenergic system. J Comp Neurol 415:145–159.

Koob GF. 1999. Corticotropin-releasing factor, norepinephrine, and stress. Biol Psychiatry 46:1167–1180.

Lin L, Faraco J, Li R, Kadotani H, Rogers W, Lin X, Qiu X, de Jong PJ, Nishino S, Mignot E. 1999. The sleep disorder canine narcolepsy is caused by a mutation in the hypocretin (orexin) receptor 2 gene. Cell 98:365–376.

Loewy AD. 1991. Forebrain nuclei involved in autonomic control. Prog Brain Res 87:253–268.

Marcus JN, Aschkenasi CJ, Lee CE, Chemelli RM, Saper CB, Yanagisawa M, Elmquist JK. 2001. Differential expression of orexin receptors 1 and 2 in the rat brain. J Comp Neurol 435:6–25.

McDonald AJ. 1992. Cell types and intrinsic connections of the amygdala. In: Aggleton JP, editor. The amygdala: neurobiological aspects of emotion, memory, and mental dysfunction. New York: Wiley-Liss Inc. p 67–96.

Moga MM, Saper CB, Gray TS. 1989. Bed nucleus of the stria terminalis: cytoarchitecture, immunohistochemistry, and projection to the parabrachial nucleus in the rat. J Comp Neurol 283:315–332.

Moga MM, Weis RP, Moore RY. 1995. Efferent projections of the paraventricular thalamic nucleus in the rat. J Comp Neurol 359:221–238.

Nishino S, Ripley B, Overeem S, Lammers GJ, Mignot E. 2000. Hypocretin (orexin) deficiency in human narcolepsy. Lancet 355:39–40.

Pacak K, McCarty R, Palkovits M, Kopin IJ, Goldstein DS. 1995. Effects of immobilization on in vivo release of norepinephrine in the bed nucleus of the stria terminalis in conscious rats. Brain Res 688:242–246.

Paxinos G, Watson C. 1998. The rat brain in stereotaxic coordinates. San Diego: Academic Press.

Peyron C, Tighe DK, van den Pol AN, de Lecea L, Heller HC, Sutcliffe JG, Kilduff TS. 1998. Neurons containing hypocretin (orexin) project to multiple neuronal systems. J Neurosci 18:9996–10015.

Piper DC, Upton N, Smith MI, Hunter AJ. 2000. The novel brain neuropeptide, orexin-A, modulates the sleep-wake cycle of rats. Eur J Neurosci 12:726–730.

Rosin DL, Talley EM, Lee A, Stornetta RL, Gaylinn BD, Guyenet PG, Lynch KR. 1996. Distribution of alpha 2C-adrenergic receptor-like immunoreactivity in the rat central nervous system. J Comp Neurol 372:135–165.

Sakurai T, Amemiya A, Ishii M, Matsuzaki I, Chemelli RM, Tanaka H, Williams SC, Richarson JA, Kozlowski GP, Wilson S, Arch JR, Buckingham RE, Haynes AC, Carr SA, Annan RS, McNulty DE, Liu WS, Terrett JA, Elshourbagy NA, Bergsma DJ, Yanagisawa M. 1998. Orexins and orexin receptors: a family of hypothalamic neuropeptides and G protein-coupled receptors that regulate feeding behavior. Cell 92:573–585.

Schwaber JS, Kapp BS, Higgins GA, Rapp PR. 1982. Amygdaloid and basal forebrain direct connections with the nucleus of the solitary tract and the dorsal motor nucleus. J Neurosci 2:1424–1438.

Sofroniew MV. 1983. Direct reciprocal connections between the bed nucleus of the stria terminalis and dorsomedial medulla oblongata: evidence from immunohistochemical detection of tracer proteins. J Comp Neurol 213:399–405.

Swanson LW, Hartman BK. 1975. The central adrenergic system. An immunofluorescence study of the location of cell bodies and their efferent connections in the rat utilizing dopamine-beta-hydroxylase as a marker. J Comp Neurol 163:467–505.

Swanson LW, Petrovich GD. 1998. What is the amygdala? Trends Neurosci 21:323–331.

Talley EM, Rosin DL, Lee A, Guyenet PG, Lynch KR. 1996. Distribution of alpha 2A-adrenergic receptor-like immunoreactivity in the rat central nervous system. J Comp Neurol 372:111–134.

Thannickal TC, Moore RY, Nienhuis R, Ramanathan L, Gulyani S, Aldrich M, Cornford M, Siegel JM. 2000. Reduced number of hypocretin neurons in human narcolepsy. Neuron 27:469–474.

Trivedi P, Yu H, MacNeil DJ, Van der Ploeg LH, Guan XM. 1998. Distribution of orexin receptor mRNA in the rat brain. FEBS Lett 438:71–75.

Watts AG, Swanson LW, Sanchez-Watts G. 1987. Efferent projections of the suprachiasmatic nucleus: I. Studies using anterograde transport of Phaseolus vulgaris leucoagglutinin in the rat. J Comp Neurol 258:204–229.

Weaver DR, Rivkees SA, Reppert SM. 1989. Localization and characterization of melatonin receptors in rodent brain by in vitro autoradiography. J Neurosci 9:2581–2590.

Williams LM, Martinoli MG, Titchener LT, Pelletier G. 1991. The ontogeny of central melatonin binding sites in the rat. Endocrinology 128:2083–2090.

Woulfe JM, Flumerfelt BA, Hrycyshyn AW. 1990. Efferent connections of the A1 noradrenergic cell group: a DBH immunohistochemical and PHA-L anterograde tracing study. Exp Neurol 109:308–322.

Zaborszky L, Cullinan WE. 1996. Direct catecholaminergic-cholinergic interactions in the basal forebrain. I. Dopamine-beta-hydroxylase- and tyrosine hydroxylase input to cholinergic neurons. J Comp Neurol 374:535–554.